coatings

MDPI

Article

PTFE-Containing Coating Obtained on Ti by Spraying and PEO Pretreatment

Dmitry V. Mashtalyar, Arina I. Pleshkova, Mariia A. Piatkova *, Konstantine V. Nadaraia, Igor M. Imshinetskiy, Evgeny A. Belov, Sergey N. Suchkov, Sergey L. Sinebryukhov and Sergey V. Gnedenkov

Institute of Chemistry FEB RAS, Vladivostok 690022, Russia
* Correspondence: piatkova.mariia.al@gmail.com

Abstract: In case of using titanium alloys in equipment exposed to aggressive media (for example, sea water), it is necessary to take into account and, first of all, prevent the formation of a galvanic couple of titanium and another metal/alloy, which in most cases leads to the corrosion destruction of the latter. Another significant problem of using titanium is its low wear-resistance and poor tribological characteristics. To impart the necessary properties to titanium and its alloys, a composite coating was formed on the top of titanium. For the coating formation, a combination of the plasma electrolytic treatment and polymer spraying was used. The SEM, EDS and XRD analyses established morphological features, elemental and phase composition of the composite coatings. Contact angles and the wettability parameters of the composite coatings were investigated. An analysis of the data obtained showed that composite coatings have better protective properties than untreated material and base PEO coatings.

Keywords: plasma electrolytic oxidation; titanium; composite coating; superdispersed polytetrafluoroethylene; protective coatings

check for updates

Citation: Mashtalyar, D.V.; Pleshkova, A.I.; Piatkova, M.A.; Nadaraia, K.V.; Imshinetskiy, I.M.; Belov, E.A.; Suchkov, S.N.; Sinebryukhov, S.L.; Gnedenkov, S.V. PTFE-Containing Coating Obtained on Ti by Spraying and PEO Pretreatment. *Coatings* **2023**, *13*, 1249. https://doi.org/10.3390/coatings13071249

Academic Editor: Cecilia Bartuli

Received: 15 June 2023
Revised: 6 July 2023
Accepted: 12 July 2023
Published: 14 July 2023

Copyright: © 2023 by the authors. Licensee MDPI, Basel, Switzerland. This article is an open access article distributed under the terms and conditions of the Creative Commons Attribution (CC BY) license (https://creativecommons.org/licenses/by/4.0/).

1. Introduction

At present, titanium and its alloys are increasingly being used as structural and functional materials in various industries. However, there are a number of disadvantages that limit their use.

The corrosion-resistance of titanium is due to the formation of a strong oxide film on the titanium surface, which prevents its destruction. Therefore, the use of titanium and titanium alloys is widespread in industries where high corrosion-resistance is required [1]. Nevertheless, it should be noted that the exceptional corrosion-resistance of titanium and its alloys is often not only an advantage but also a disadvantage, which is associated with a high probability of the formation of a galvanic couple when the titanium/titanium alloy is in the presence of other metal materials (copper, some steels, etc.) in a corrosive environment. This can lead to a fairly rapid destruction of the contacting metal, and, as a consequence, the loss of the functional reliability of the entire system [2,3]. An additional factor limiting the use of titanium and titanium alloys is the high value of elastic deformation and low thermal conductivity of these materials [3].

To date, there is an extensive list of methods of protection from the effects of negative damaging factors. Thus, in most cases, reagent methods for treating a corrosive-active medium are used in industry to reduce corrosion losses, for example, by adding inhibitors. Other methods of metals protection are possible: alloying, special structural solutions, and electrochemical protection. One of the possible highly efficient ways to protect products from the negative impact of the environment is coatings formation [4–6]. The main advantage in comparison with bulk methods in this case is the possibility of maintaining the original advantages of the processed material, since only the surface layer is subjected to modification.

Plasma electrolytic oxidation (PEO) can be singled out among a wide variety of methods for forming coatings on titanium and its alloys [7]. The coatings obtained by PEO have high corrosion-resistance, significant wear-resistance and high adhesion to the substrate due to the formation of chemical bonds between the coating and the base material [8]. Moreover, we note that the surface layers synthesized by this type of plasma electrolytic treatment have a special structure. For example, a PEO coating consists of an inner, almost poreless sublayer, which is mainly responsible for corrosion properties, and an outer developed porous layer, which characterizes the mechanical properties of the coating [8]. The presence of pores of micron size and smaller in the composition of the formed coating [3] allows us to consider it as a suitable basis for the introduction of various—including nanosized—substances that significantly improve the protective properties of the coating [9].

A promising strategy, as noted above, is the use of a PEO layer as a base for creating composite coatings, including polymer-containing coatings [10]. In this case, it is possible to impart new functionally significant properties to the coating. Tsai et al. [11] succeeded in imparting hydrophobic properties to the surface by applying fluoropolymers to the PEO layer. However, it should be noted that the maximum values of the contact angle (CA) for such polymer-containing layers were only 129.9° ± 9.4° [11]. In another work [12], on the contrary, hydrophilic coatings were formed on the titanium alloy Ti6Al4V due to the combination of PEO and polymers. The use of hydrophilic polymers made it possible to improve the wear-resistance of coatings [12]. The authors note that such composite layers can be further used as a way to reduce the wear of titanium implants. However, more in vivo studies are required to clarify the effect of such coatings on surrounding body tissues.

To increase the wear-resistance, Martini et al. used PEO followed by the application of polytetrafluoroethylene (PTFE) [11]. As a result of tribological studies, it has been established that such polymer-containing coatings significantly reduce material wear by imparting antifriction properties to the surface [12]. The authors of [13] used polyethylene oxide as the polymer component of the composite layer. The formed coatings demonstrated high corrosion-resistance to long-term (1-month) exposure to an aggressive environment. The achievement of such an effect is attributed by the authors, among other things, to a decrease in the porosity of the coatings [14].

The use of composite coatings formed as a result of such a combination would not only improve the performance characteristics of processed materials but also expand the scope of their application.

In our previous paper [1], we have obtained composite coatings on titanium using PTFE. However, the hydrophobicity of these layers requires improvement. Thus, based on our studies devoted to the formation of superhydrophobic surfaces on magnesium alloys [15], in this work, for the improvement of the hydrophobicity of protective coatings, we have decided to use a combination of PEO treatment and the subsequent incorporation of PTFE to the PEO layer by spraying. Detailed studies of the composition, morphological features, wettability, and protective properties of obtained surfaces were carried out. To the best of our knowledge, such a study has never been performed before.

2. Materials and Methods

2.1. Samples

The samples were prepared using rectangular plates made of VT1-0 commercial pure titanium (Ti content 99.24%–99.7%) (15 × 20 × 1 mm^3). Before the formation of coatings, all samples were polished with sandpaper (up to P1000), washed with distilled water, and degreased with alcohol.

2.2. Coatings Formation

In this work, the mode of plasma electrolytic oxidation was chosen taking into account previous studies on the formation of coatings on titanium alloys [16–26], in which

a two-stage monopolar mode was used. At the first stage, a potentiodynamic increase in voltage was carried out for 120 s, due to which an anode oxide layer is first formed on the surface, with the subsequent appearance of the first sparks on the surface of the sample being processed. At the second stage, the voltage decreased potentiodynamically over 580 s, which contributed to the formation of a denser PEO layer with a developed surface morphology. Then, all samples were washed with distilled water, degreased with alcohol, and dried with warm air. The electrolyte's composition includes sodium phosphate (Na_3PO_4) at a concentration of 25 g/L.

2.3. Composite Coatings Formation

The formation of composite coatings was conducted using Forum® superdispersed polytetrafluoroethylene (SPTFE) (Institute of Chemistry FEB RAS, Vladivostok, Russia) obtained by the method of the thermogradient synthesis of fluoroplast-4 (MITO, Kirovo-Chepetsk, Russia). The size of the SPTFE powder particles ranged from 0.2 to 1.5 μm (average size is 0.35 μm). In order to increase the manufacturability of applying the composite layer, we used a 10% suspension of SPTFE powder in isopropanol [7].

As a processing method, the spray-coating method was used, the essence of which is to apply the required substance using a directed flow to the surface of metals and alloys. Spraying of SPTFE was carried out by air at a decreasing pressure from 0.6 to 0.4 MPa. The distance from the nozzle to the surface of the workpiece was about 20 cm. After applying the polymer, the samples were dried in air for 10–15 min until the complete evaporation of isopropanol. After drying, the samples were heat-treated in a muffle furnace at a special temperature mode (315 °C) for 15–30 min. They were then cooled together with the furnace [7].

A description of each sample type and their corresponding designation is provided in Table 1.

Table 1. Description of the studied samples and corresponding designation.

Sample	Designation
Bare titanium	Ti
PEO coating	PEO
PEO coating with SPTFE (composite coating)	CC

To study the influence of the amount of sprayed fluoropolymer material, SPTFE was applied one (CC-1x), two (CC-2x) and three (CC-3x) times on the base PEO coating.

2.4. Analysis of Coatings Composition and Morphology

An EVO 40 scanning electron microscope (Carl Zeiss, Oberkochen, Germany) with an INCA X-act instrument (Oxford Instruments, Abingdon, UK) for energy dispersive spectroscopy (EDS) was used to study surface morphology and cross-sections and analyze the elemental composition of the coatings. Before analysis, a thin layer (100 nm) of Cr was sprayed onto the samples. The sprayed film provided sufficient electrical conductivity to the samples' surface layer, which is necessary to prevent the formation and accumulation of electric charge on their surface.

The phase composition of the formed surface layers was determined in the "Far East Center for Structural Research" on a SmartLab X-ray diffractometer (XRD) (Rigaku, Tokyo, Japan), using Cu-Kα radiation. During the analysis, Bragg–Brentano geometry focusing was used in the 2θ angle range from 10° to 80° with a step of 0.02° and an exposure time of 1 s at each point. During XRD analysis, the "EVA" search program with the "PDF-2" data bank was used.

2.5. Electrochemical Properties of Coatings

The corrosion studies of the samples were carried out by potentiodynamic polarization and electrochemical impedance spectroscopy (EIS) using the VersaSTAT MC electrochemical

system (Princeton Applied Research, Oak Ridge, TN, USA). The measurements were carried out in a three-electrode cell at room temperature in a 3.5% NaCl solution. A platinized niobium mesh was used as a counter electrode. A saturated calomel electrode (SCE) was used as a reference electrode. The area of the sample immersed in corrosion medium was 1 cm^2. Before electrochemical experiments, the open circuit potential (OCP) was measured for 15 min. During the EIS test, the sinusoidal signal had an amplitude of 10 mV (rms). The electrode potential was stabilized in the frequency range from 0.01 Hz to 0.1 MHz with a logarithmic sweep of seven points per decade.

Potentiodynamic measurements were performed with a potential sweep rate of 1 mV/s in the range from $E_C - 0.15$ V to $E_C + 0.50$ V. The Levenberg–Marquardt method was used for obtaining a more accurate experimental dependence of the current density I over potential E (Equation (1)) [27–29]:

$$I = I_C(10^{\frac{E-E_C}{\beta_a}} + 10^{-\frac{(E-E_C)}{\beta_c}}) \quad (1)$$

This type of method makes it possible to obtain the best-fit values of corrosion potential E_C, corrosion current density I_C, the slope of the cathodic polarization curve β_c, and the slope of the anodic polarization curve β_a.

The polarization-resistance R_P was determined with the potentiodynamic polarization of the sample in the potential region $\Delta E = E_C \pm 20$ mV with a scan rate of 0.167 mV/s, in which the linear dependence $I = f(E)$ is observed (Equation (2)):

$$R_P = \frac{\Delta E}{\Delta I} \quad (2)$$

2.6. Assessment Adhesion Characteristics

The adhesion strength of the coatings was evaluated using a Revetest Scratch Tester (CSM Instruments, Peseux, Switzerland).

The study of adhesion was carried out by measuring the critical load at which the delamination of the composite or base PEO layer occurred. The indenter was a Rockwell conical diamond tip with a tip angle of 120° and a radius of curvature equal to 200 μm. The length of movement of the indenter along the sample's surface was equal to 5 mm; the maximum applied load was equal to 20 N.

During the tests, the physical parameters were recorded according to the applied load and the length of the scratch.

2.7. Wettability of Coatings

The hydrophobic or hydrophilic properties of the samples were studied by the sessile drop method on a DSA100 goniometer (Krüss, Hamburg, Germany). This method allows us to measure the optical contact angle (CA). The angle between the drop base line and the tangent to the drop boundary at the contact point of the three phases was measured according to [30].

Distilled water was used as a test liquid; the drop volume was 5 μL. In this work, the Young–Laplace fit was used to calculate the CA [31,32]. With this fit, the parameters of the system of equations simulating the shape of a sessile drop are determined by numerical analysis. In addition, contact angle hysteresis (CAH) was measured for samples with composite coatings.

3. Results and Discussion

3.1. Formation PEO Coating on VT1-0 Commercially Pure Titanium

One of the criteria necessary for the formation of composite coatings, as noted above, is the presence of a developed surface morphology and the porous structure of the base PEO layer [17–21]. The presence of the structure described above makes it possible to introduce the fluoropolymer material into the PEO layer.

For titanium and titanium alloys, the composition and concentration of the electrolyte have a special effect on the properties of the formed coating. In order to obtain coatings with different properties, many research groups have considered the influence of changes in the electrolyte's composition and its effect on the formed PEO layers [19–26].

We also note that the concentration of electrolyte elements has a greater effect not only on the composition of the resulting PEO coating but also on the course of the process itself. According to the results of the studies, the concentration of sodium phosphate (Na_3PO_4), chosen as the main component of the electrolyte, had a direct effect on the parameters of the PEO process (Figure 1).

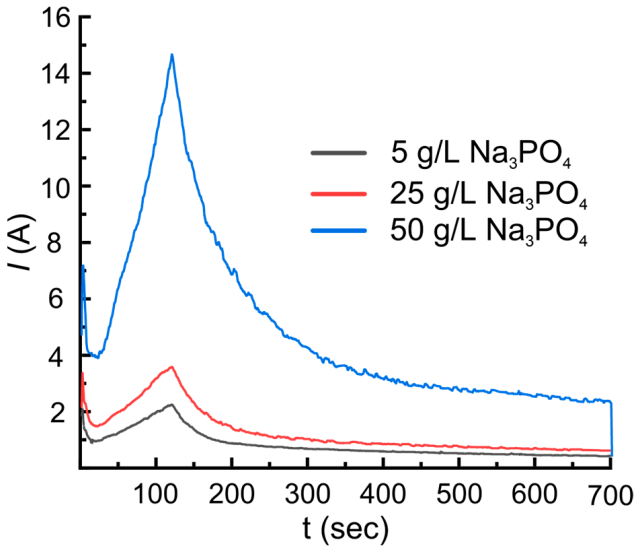

Figure 1. Changes in current strength during PEO on VT1-0 titanium at different concentrations of sodium phosphate.

At a sodium phosphate concentration of 25 g/L, the oxidation process proceeds actively, with a significant formation of sparks on the sample surface. The highest concentration of sparks is noted on the faces of the sample, which become points of stress concentration. The PEO layer formed under these conditions has a developed morphology and a thickness of about 15–20 μm.

A lower concentration of electrolyte elements does not contribute to the ignition of a plasma discharge on the surface of the material being processed. In this case, the current strength is insufficient to form a surface layer of the required thickness. The coating obtained at low electrolyte concentrations is thin, does not exceed 3–5 μm, has a less developed structure (Figure 2), and therefore is not suitable for forming composite layers on its basis.

At a high concentration of electrolyte elements, about 50 g/L, a more active formation of arc discharges occurs during the oxidation process, which, due to their large number and power, destroy the resulting protective coating and lead to the destruction of metal products at the edges—at points of stress concentration (Figure 2). From the resulting plot of the coating's formation during plasma electrolytic oxidation, it can be concluded that the current strength that occurs during oxidation in highly concentrated electrolytes has significantly higher values than in the case of using an electrolyte with a Na_3PO_4 concentration of 25 g/L (Figure 1). In this case, the electrolyte has a high resistance, which causes a rapid increase in the intensity and the formation of a powerful arc discharge, which leads to the destruction of both the oxide layer being formed and the substrate material itself.

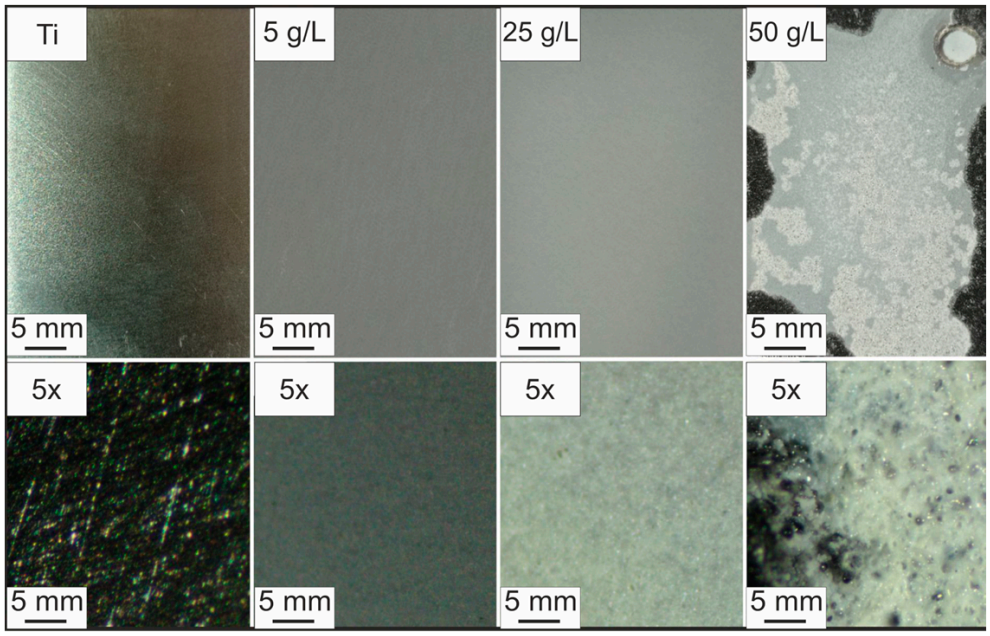

Figure 2. Optical images of samples with surface layers formed on VT1-0 titanium in electrolytes with different concentrations of sodium phosphate.

Another factor influencing the formation of the protective layer is the given conditions of the formation process. The influence of a given voltage in the system determines the process of charge accumulation on the metal surface. With too slow an accumulation on the surface, a short-lived spark discharge is not formed, which does not start the process of formation of a porous PEO layer. With too rapid an accumulation of tension, spark discharges, on the contrary, are formed more actively, causing the destruction of the resulting protective layer.

In this study, the maximum values of stresses in the system were changed, due to which the appearance and state of the formed coating changed.

Reducing the voltage limit to 140 V or 170 V promotes the formation of a coating with low roughness, effectively bringing the PEO process to conventional anodizing. The outer oxide layer is thin and smooth (Figure 3). The thickness of such a coating was 10–15 μm, which is insufficient in the case of using a PEO layer as a basis for the formation of a composite material. In this case, the resulting coating has a flat smooth surface (Figure 3). However, in the samples obtained at 170 V, the formation of micropores is observed, the presence of which is due to the appearance of the first spark discharges during PEO.

When the formation voltage is increased to 370 and 400 V, the coating is obtained with a developed surface morphology and a large number of pores, but of small thickness (Figure 3). This is due to the formation of powerful plasma discharges on the surface of the processed sample, which, due to their power, destroy the resulting oxide layer. This is especially noticeable for the sample, the PEO of which was carried out at 400 V. On the surface, there are obvious defects (black dots), indicating the destruction of the coating as a result of the flow of powerful plasma discharges during oxidation (Figure 3). The most optimal mode for coating formation is that in which the maximum voltage reaches 270 V. For such coatings, as indicated above, along with acceptable protective characteristics, a developed surface morphology is observed, suitable for the formation of composite polymer-containing layers (Figure 3).

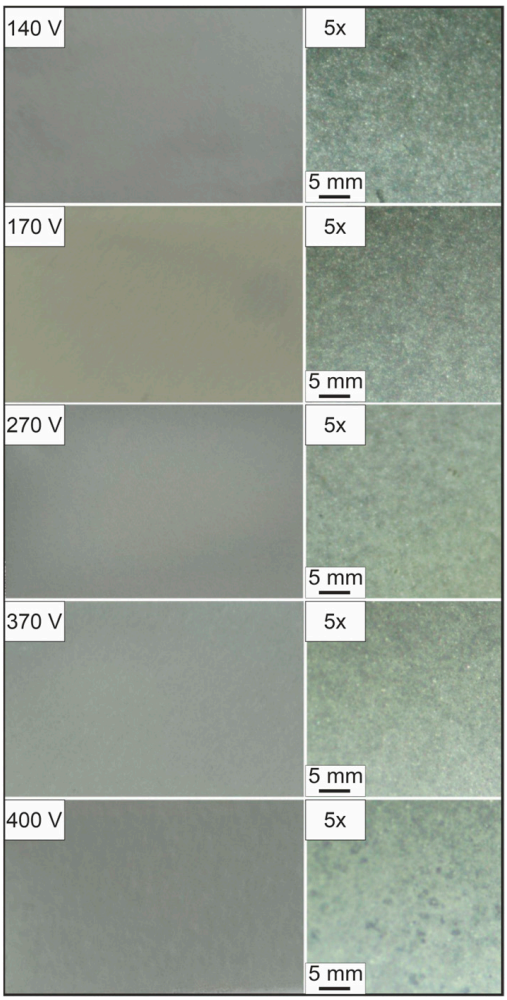

Figure 3. Optical images of PEO coatings formed on VT1-0 titanium at various voltage values.

3.2. Formation of Composite Coatings by Spray-Coating

Preliminary tests established the optimal aerosol method for applying organofluorine material [17] using a medium-pressure compressor and a spray gun. Spraying was carried out with air at a pressure decrease from 0.6 to 0.4 MPa. Such values of pressure during surface treatment initially make it possible to incorporate polymer particles into the pores of the coating and obtain a uniform layer due to particle deformation (Figure 4). A gradual decrease in pressure is necessary since at such a mode the sprayed particles do not destroy the polymer that has already reached the surface, but adhere to it, increasing the layer thickness. The distance between the nozzle and the surface was about 20 cm, and while at least 90% of the sprayed material falls on the surface, the rest disappears.

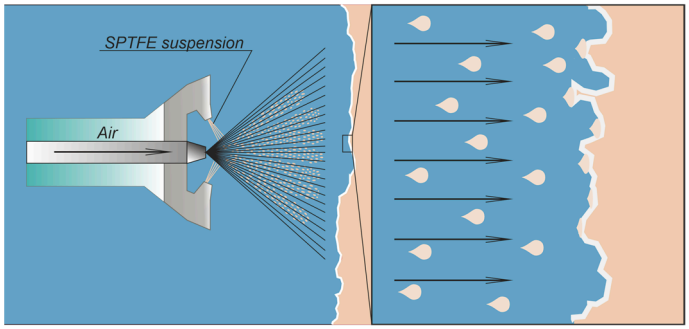

Figure 4. Scheme of formation of composite coatings on metals and alloys by spray coating.

After applying the polymer, the samples were dried in air for 10–15 min until the complete evaporation of isopropyl alcohol. This is necessary so that during further heat treatment the alcohol does not boil, thus forming defects in the polymer film. After drying, the samples are thermally treated in a muffle furnace at a temperature regime (315 °C for 15–30 min, cooling together with the furnace).

During heat treatment, the SPTFE softens and reaches a fluidity sufficient to penetrate the porous part of the coating without the formation of defects. Gradual cooling increases the proportion of crystalline PTFE and prevents it from cracking during the glass transition.

According to the literature data and the analysis of many technological processes, this processing method in comparison with others is quite simple and does not require special qualifications of the operator and expensive equipment. It allows us to reduce the consumption of the substance and process surfaces of various sizes and complexities, including large-sized products; has a lesser impact on the environment; and is implemented in almost any conditions.

Studies regarding the effect of the volume of the sprayed substance on the composition, structure, and quality of composite coatings formed by the method described above were carried out in this work. Thus, three types of coatings were obtained with different volumes of introduced dispersions. Data on the correspondence of the designation of coatings and the volume of the suspension used are given in Table 2.

Table 2. Designation of composite coatings.

Designation	CC-1x	CC-2x	CC-3x
Volume of dispersion, mL/cm^2	0.35	0.65	0.95

Figure 5 shows optical images of bare titanium, PEO coating, and composite coatings CC-1x, CC-2x, and CC-3x (Table 2). An analysis of the image data allows us to conclude that the formed coatings are quite uniform and do not have visible defects, with the exception of CC-3x. This coating is not composite, since, most likely, due to excess polymer, a thick film is formed, the thermal treatment of which leads to the cracking and flaking of polymer from the PEO coating.

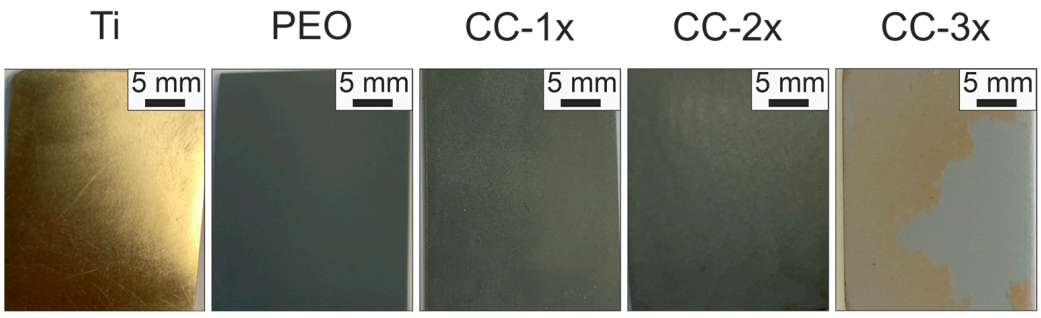

Figure 5. Optical images of materials without coating, with PEO and composite coatings: CC-1x, CC-2x and CC-3x.

Also, from the assessment of the appearance of the coatings, it can be concluded that the larger the volume of the sprayed material, the darker the surface becomes, which is indirect evidence of an increase in the thickness of the polymer film and is confirmed by the data in Table 3. The increase in the coating thickness is about 1–2 microns, depending on the volume of the sprayed substance.

Table 3. Thickness and porosity of PEO and composite coatings.

Parameters	d [1], μm	Ps [2], %	Pcs [3], %
PEO	7	14.45	4.40
CC-1x	7	-	3.81
CC-2x	8	-	3.76
CC-3x	10	-	3.58

[1] d—thickness of the coatings, [2] Ps—surface porosity, [3] Pcs—cross section porosity.

3.3. Composition and Morphology of Coatings

The surface morphology and microrelief were studied by the OSP370 optical surface profilometry method using an instrument installed on an M370 workstation (Princeton Applied Research, Oak Ridge, TN, USA). Scanning speed 150 μm/s in 1 μm increments. Data analysis was performed using Gwyddion 2.45 software. To quantify the surface roughness, three-dimensional parameters *Sa*, *Sq* were used, where: *Sa* is the arithmetic mean deviation of the surface; *Sq* is the standard deviation of the surface from the base plane.

An analysis of the roughness and characteristic parameters presented in Table 4 showed that the application of superdispersed polytetrafluoroethylene to the PEO layer changes the state of the surface. During the formation of the composite coating, the fluoropolymer penetrates into the pores of the PEO layer and seals them.

Table 4. Surface roughness parameters with composite coatings.

Sample	Sa, μm	Sq, μm
PEO	2.0	2.4
CC-1x	1.5	1.8
CC-2x	1.2	1.5
CC-3x	1.1	1.3

An analysis of the data of the SEM images presented in Figure 6 shows the significant change in coatings morphology after spraying SPTFE particles onto the base PEO. However, at a volume of 0.95 mL/cm^2, defect formation is observed in the polymer film. The SEM image of the CC-3x titanium alloy (Figure 6) shows the reason for the delamination of the polymer film from the base PEO coating. The surface roughness of the PEO coating on titanium alloy is low and the porosity is small, mainly due to the small pore size, as a result of which a small amount of polymer becomes quite sufficient to cover the surface with a thin polymer film. A further increase in the amount of the sprayed suspension leads to an increase in thickness and, consequently, to an increase in internal stresses, resulting in the appearance of cracks in the composite coating during heat treatment. This circumstance leads to a decrease in the adhesion of the polymer film and its delamination from the matrix.

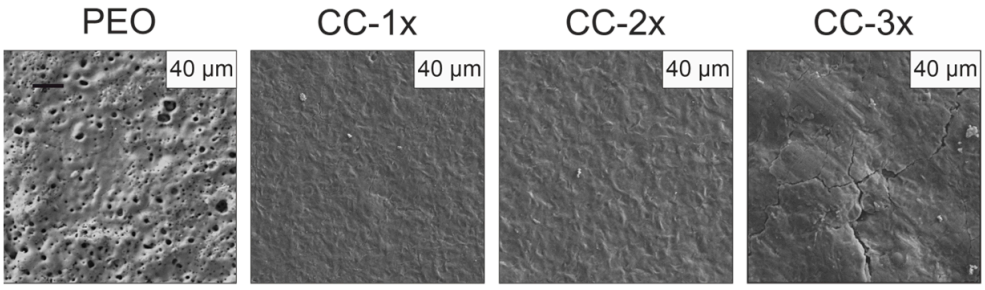

Figure 6. SEM images of the surface of PEO- and composite coatings on titanium alloy.

The results of EDS analysis (Figure 7) made it possible to establish the distribution of elements in the coating and on its surface. Thus, the presence of titanium (Ti), oxygen (O), and phosphorus (P) in the composition of the PEO coating is observed, distributed over the

entire thickness and surface of the coating, while fluorine (F) and carbon (C) are present only in the upper layer, which confirms the presence of organofluorine compounds in the composition of the composite coating (Figure 7). The distribution of phosphorus (P) over the entire thickness of the coating is explained by the oxidation of the titanium alloy in a phosphate electrolyte with a high content of sodium phosphate (Na_3PO_4).

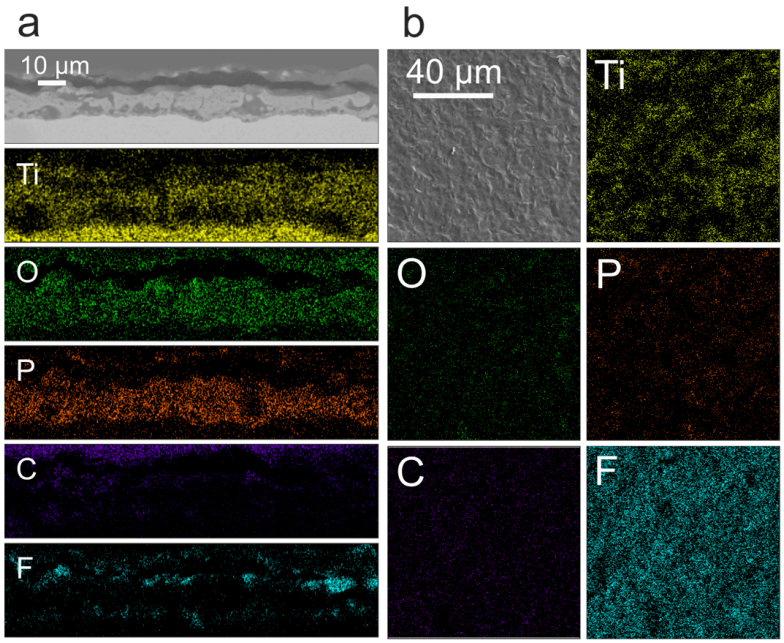

Figure 7. Results of EDS of composite coatings on titanium alloy: maps of elements distribution over the coatings thickness (**a**) and on top layer (**b**).

The phase composition of the formed coatings was determined by XRD (Figure 8). For formed composite coatings, there is an increase in the intensity of the SPTFE peak and a decrease in the intensities of the lines of phases that are part of the PEO coatings (TiO_2 as a rutile and anatase) (Figure 8).

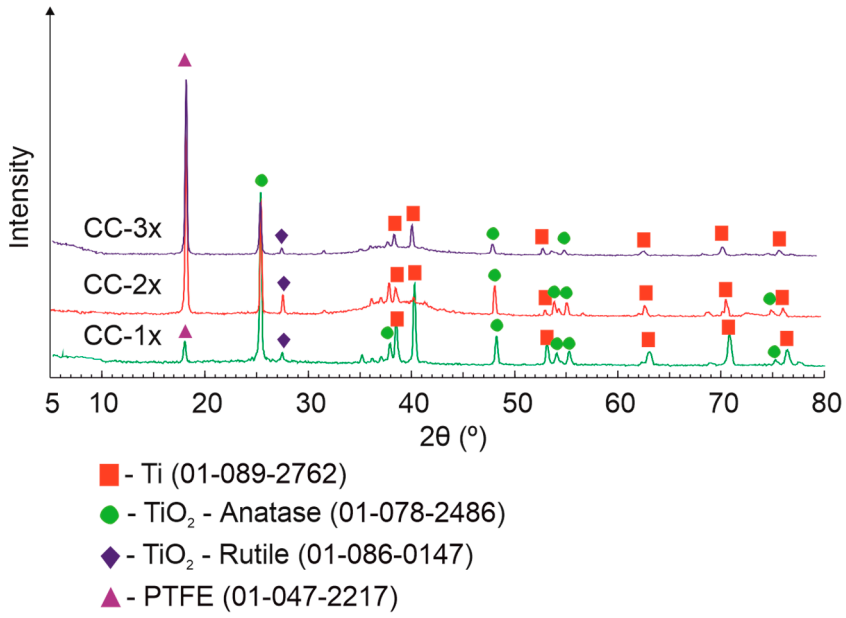

Figure 8. X-ray diffraction patterns of composite coatings on titanium alloy.

During the PEO process, a metastable TiO_2 phase (anatase) was formed (Figure S1, JCPDS Card No: 01-078-2486) along with TiO_2 (rutile) (Figure S1, JCPDS Card No: 01-086-0147). The presence of this phase is typically for PEO layers formed on titanium material. The formation of these phases is the result of thermochemical and plasmachemical reactions occurring at the electrode/electrolyte interface. Thus, despite the high temperature of plasma microdischarges (up to 10,000 °C) [1,9], these microdischarges are short-lived (no more than 200 µs), and after their attenuation, the breakdown zone is sharply cooled to the electrolyte temperature. This process reduces the probability of the formation of a stable high-temperature rutile phase [9]. Summarizing the above, two TiO_2 phases are presented in the base PEO coating (Figure S1).

Also, the XRD pattern of the composite coating has a peak of PTFE at 18°, (Figure S1, JCPDS Card No: 01-047-2217). This is due to the presence of PTFE within the crystalline structure in the composite coating. The crystalline phase of PTFE occurred due to the thermal treatment of the polymer-containing layer (315 °C).

The presence of titanium lines on the XRD patterns (Figure S1, JCPDS Card No: 01-089-2762) is due to the low absorbing capacity of the formed layers and the penetration of X-rays into the substrate during the analysis.

Thus, summarizing the data of XRD and EDS, we can conclude that on the basis of PEO coatings, as a result of treatment with SPTFE by spray-coating, composite coatings were obtained with a high content of crystalline polytetrafluoroethylene (Figure 8), which was embedded in the outer porous layer of PEO coatings (Figures 6 and 7).

3.4. Electrochemical Properties of Coatings

The corrosion properties of the samples with different types of treatment were investigated by potentiodynamic polarization tests. According to the data obtained (Figure 9, Table 5), uncoated titanium has high corrosion-resistance. This is due to the effect of the passivation and self-passivation of titanium and titanium alloys. The passivation of titanium occurs particularly rapidly in an environment in which oxidizing agents, primarily oxygen, are present. In this case, an oxide film Ti_xO_y is formed on the titanium surface, which protects it from corrosion damage.

The formation of a PEO coating on the surface of the titanium alloy significantly reduces the corrosion current density I_C and increases the polarization-resistance R_P (Figure 9, Table 4), which significantly reduces the corrosion of the processed material. An evaluation of the data of the electrochemical tests indicates the positive effect of incorporating polytetrafluoroethylene into the PEO coating (Figure 9). According to the presented data, a single application of SPTFE reduces the corrosion current density in comparison with the PEO coating (Table 5) [17].

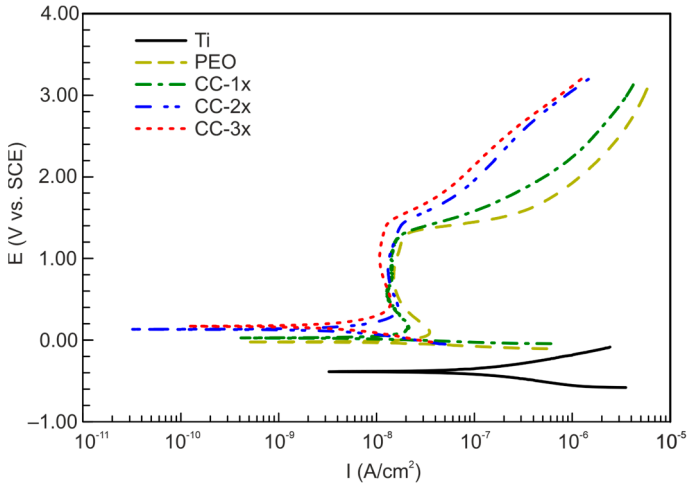

Figure 9. Polarization curves for samples with different types of surface treatment.

Table 5. Corrosion properties (corrosion potential E_C, corrosion current density I_C, polarization-resistance R_P) of samples with different types of surface treatment.

Sample	E_C (V vs. SCE)	I_C (A/cm^2)	R_P ($\Omega \times$ cm^2)
Ti	–0.38	1.3×10^{-7}	3.5×10^{5}
PEO	–0.07	1.7×10^{-8}	1.1×10^{6}
CC-1x	0.03	1.6×10^{-8}	1.6×10^{6}
CC-2x	0.13	8.2×10^{-9}	7.2×10^{6}
CC-3x	0.13	7.2×10^{-9}	9.5×10^{6}

A subsequent increase in the amount of fluoropolymer material introduced into composite coatings makes it possible to increase the protective properties of composite structures (Table 4). Thus, an increase in protective characteristics occurs in the series PEO → CC-1x → CC-2x → CC-3x.

EIS data are presented in the form of Bode plots (dependences of the impedance modulus $|Z|$ and phase angle θ on frequency f). Based on the analysis of the EIS results (Figure 10), it can be concluded that the multiplicity of treatment with SPTFE of the base PEO layer has significant effect on the nature of charge transfer at the electrode/electrolyte interface.

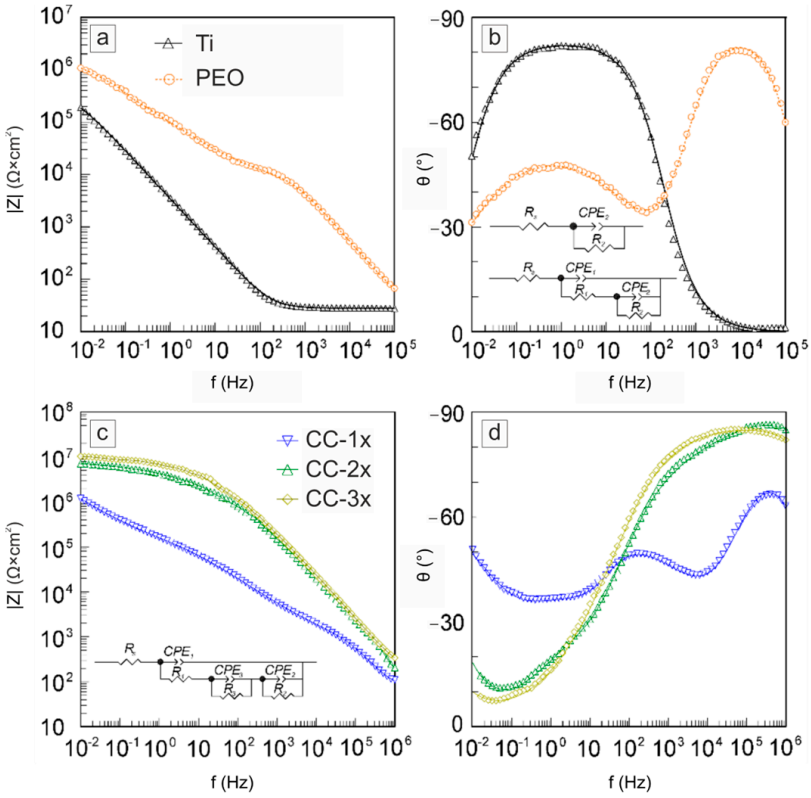

Figure 10. Bode plots (dependence of impedance modulus $|Z|$ (**a**,**c**) and phase angle θ (**b**,**d**) of frequency f) for samples with different types of surface treatment. The symbols indicate the experimental data, and the lines is the fitting curves calculated in accordance with the proposed models.

The spectrum for an uncoated sample can be described using an electrical equivalent circuit with a single *R–CPE* chain (Figure 10b), where R_2 is the charge transfer-resistance and CPE_2 is the capacitance of the natural oxide layer. The dependence of the phase angle on frequency for the uncoated sample has a bend in the mid-frequency region, which is common for such metal surfaces.

The spectrum for PEO coatings was described using a two *R-CPE* chains (Figure 10b), where the R_2-CPE_2 element characterizes the inner pore-free sublayer of the PEO coating and R_1-CPE_1 characterizes the outer porous layer. The same equivalent electrical circuit (EEC) was used to describe CC-2x and CC-3x, but in these cases, R_1–CPE_1 models a porous layer filled with a polymer, and R_2–CPE_2 models an inner layer, the thickness of which increases due to the polymer located at the bottom of the pores. The spectrum for CC-1x had a non-standard shape, which was fitted using an EEC with three *R–CPE* chains (Figure 10c) due to the presence of three pronounced time constants in the Bode plot (Figure 10d).

The change in the type of the spectrum depending on the multiplicity of deposition of the composite polymer-containing layer allows us to conclude that the structure of such coatings is more complex than that of the base PEO layer. For sample CC-1x, a third time constant appears due to the sealing of pores with air by the polymer. In this case, R_1–CPE_1 characterizes the electrolyte/polymer film/air space interface, which has a high resistance R_1 to the transfer of charge (Table 6). In turn, R_3–CPE_3 is due to the presence of a polymer inside the porous part of the coating.

Table 6. Calculated parameters of equivalent electrical circuits' elements for samples with different types of surface treatment.

Sample	R_1 ($\Omega \times cm^2$)	CPE_1		R_2 ($\Omega \times cm^2$)	CPE_2		R_3 ($\Omega \times cm^2$)	CPE_3	
		Q_1 ($\Omega^{-1} \times cm^{-2} \times s^n$)	n_1		Q_2 ($\Omega^{-1} \times cm^{2} \times s^n$)	n_2		Q_3 ($\Omega^{-1} \times cm^{-2} \times s^n$)	n_3
Ti	–	–	–	3.4×10^5	5.4×10^{-5}	0.92	–	–	–
PEO	9.4×10^3	4.1×10^{-8}	0.96	2.1×10^6	3.5×10^{-6}	0.58	–	–	–
CC-1x	1.4×10^3	1.2×10^{-8}	0.88	1.9×10^4	7.7×10^{-7}	0.83	3.5×10^5	2.6×10^{-6}	0.51
CC-2x	6.2×10^4	7.2×10^{-10}	0.98	5.7×10^6	1.1×10^{-8}	0.67	–	–	–
CC-3x	1.4×10^5	1.2×10^{-9}	0.95	1.2×10^8	3.4×10^{-8}	0.38	–	–	–

For samples CC-2x and CC-3x, no third time constant is observed, which may be due to the filling of the porous part of the PEO layer with polymer and, accordingly, the absence of air in the sealed pores. This is indirectly indicated by an increase in the values of R_1 and a decrease in Q_1, which is possible with an increase in the thickness of the polymer layer (Table 6). The dynamics of changes in the values of parameters R_2 and Q_2 indicate an increase in the thickness of the non-porous sublayer of composite coatings, which is due to the penetration of the polymer to the bottom of the pores. The decrease in the values of n_2 (Table 6) for CC-2x and CC-3x is a consequence of an increase in the heterogeneity of the porous PEO layer due to the different conductivities of the polymer and PEO coating compounds, which also indicates the partial and/or complete filling of pores with SPTFE.

Based on the results of electrochemical studies, it can be established that the formation of PEO coatings on titanium alloys, followed by surface treatment with a fluoropolymer, can significantly improve the corrosion properties of these materials.

3.5. Adhesion Characteristics of Coatings

Based on the analysis of sclerometry data, it can be concluded that the process of the destruction of the base PEO layer and composite coatings under the influence of the applied load occurs according to a single mechanism: the indenter gradually penetrates into the formed coating, which is accompanied by the adhesive destruction of the surface layer (Figure 11). At the same time, depending on the type of surface treatment, there are differences in quantitative indicators.

The surface structure of PEO samples has high adhesion to the metal substrate (Table 7). The value of L_{C2} = 13.8 N, while the value of L_{C3} = 30.6 N, which indicates the high adhesion of the PEO layer (Table 7). For CC-1x, the force at which the surface layers were displaced relative to the metal substrate increased to 15.2 N, which is 10% higher than that of the base PEO coating. For CC-2x and CC-3x, the adhesion value L_{C3} is comparable within the

error and exceeds the values obtained for the PEO coating by 27%. Thus, an increase in the amount of introduced polymer allows one to increase the values of L_{C2} and L_{C3} for composite coatings. L_{C2} shows an increase in load to 19.7 N, which is 43% higher than that of the base PEO layer. Such an increase in these characteristics is caused by an increase in the amount of fluoropolymer material on the surface. The presence of PTFE in the surface structures ensures, due to the low coefficient of friction of the polymer, the sliding of the indenter, which causes an increase in the parameters under study (Figure 11).

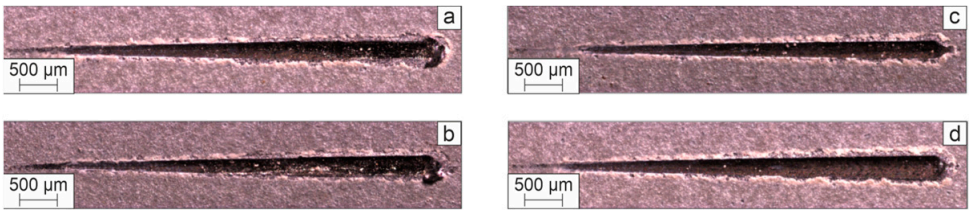

Figure 11. Optical images of a scratch deposited on the surface of a PEO coating (**a**) and composite coatings CC-1x (**b**), CC-2x (**c**), CC-3x (**d**).

Table 7. Adhesive properties of samples with different types of surface treatment.

Sample	L_{C2}, H	L_{C3}, H
PEO	13.8 ± 0.2	30.6 ± 0.4
CC-1x	15.2 ± 0.3	36.8 ± 0.4
CC-2x	18.6 ± 0.2	38.2 ± 0.5
CC-3x	19.7 ± 0.4	38.8 ± 0.6

From the previous discussion, it can be concluded that the introduced organofluorine substances have a significant effect on the adhesive properties of the created surface layers. The presence of this effect is due to the formation of composite structures containing PTFE, which have a low coefficient of friction and act as a solid lubricant when the indenter contacts the surface.

3.6. Wettability of Coatings

The results of the study of the wettability of titanium samples without coating, with PEO coating and composite coatings (CC-1x, CC-2x, CC-3x) are shown in Table 6. An analysis of these results shows that the formation of PEO coatings leads to a significant increase in wettability, which is explained by two factors. Firstly, water adsorption on oxide surfaces is much higher than on metallic ones [33], and secondly, PEO coatings have a developed surface structure, because of which the contact area of the liquid with the solid phase increases [34]. However, PEO coatings on titanium have a small pore size, as a result of which the contact angles with water for the titanium surface without and with PEO coating are identical.

The treatment of PEO coatings with a fluoropolymer leads to the appearance of hydrophobic properties at the surface (the value of the contact angle of water with the surface of the composite coatings exceeds 90°).

In this case, after a single treatment with superdispersed polytetrafluoroethylene, the previously hydrophilic PEO coating acquired hydrophobic properties, and the CA reached 131.3 ± 0.6° (i.e., up to 56° more than that for the PEO coating) (Table 8, Figure 12). However, a further increase in the number of polymer applications led to a slight decrease in the contact angle, which indicates an increase in wettability in the series CC-1x → CC-2x → CC-3x. This decrease in CA values is a consequence of a change in the morphological structure of the coatings.

Table 8. Results of CA and CAH measurements for samples with different surface treatment.

Sample	CA (°)	CAH (°)
Ti	75.1 ± 0.3	–
PEO	75.2 ± 1.4	–
CC-1x	131.3 ± 0.6	39.0 ± 0.5
CC-2x	130.2 ± 2.9	40.7 ± 0.6
CC-3x	128.1 ± 2.7	49.7 ± 0.7

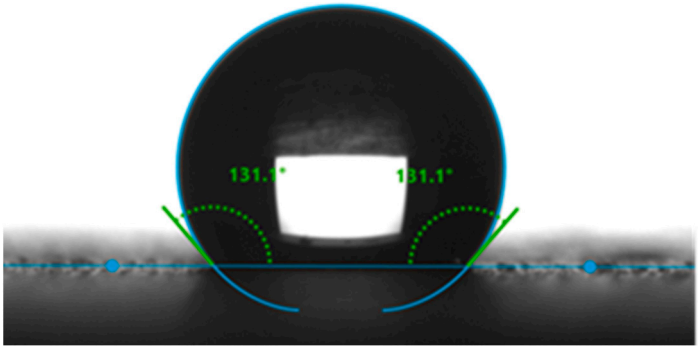

Figure 12. Optical images of a sessile drop on the surface of CC-1.

The SFE value for CC-1 is 14 mJ/m^2 (Figure 13). It can be concluded that the structure and composition of the surface of the PEO coating have a significant effect on this value. The open areas of the PEO layer and the pores not filled with polymer come into contact with the test liquids and increase the SFE.

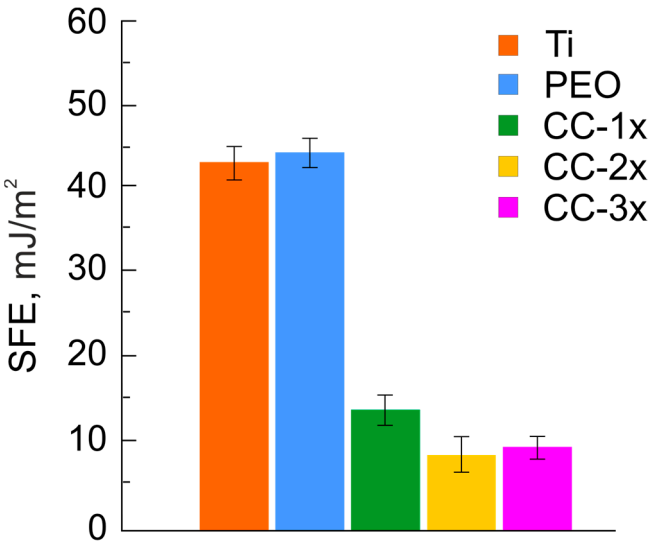

Figure 13. Dependences of the surface free energy on the substrate material and surface treatment method.

The SFE values for CC-2x and CC-3x are in the range of 8–10 mJ/m^2. It should be noted that the free energy of the smooth SPTFE surface used in this work is 14.7 mJ/m^2, which is more than 1.5 times higher than the obtained values. The substrate for the low-energy polymer layer is high energy; therefore, synergy is excluded in this case. This implies the conclusion that the boundary of contact between liquids and a solid surface is heterogeneous and is represented as the boundary of contact between a liquid and a solid surface and a liquid with air.

4. Conclusions

It can be summarized that composite coatings formed by plasma electrolytic oxidation and subsequent sputtering of organofluorine dispersions have better protective properties than untreated metal, as well as PEO coatings. We note that the best combination of protective characteristics among the studied composite coatings is CC-3x.

Thus, in the course of these studies, it was found that the corrosion current density for samples with CC-3x decreased by more than an order of magnitude in comparison with uncoated titanium and more than two times with PEO. In addition, the introduction of a fluoropolymer into the composition of the base PEO layer makes it possible to impart hydrophobic properties to the hydrophilic surface.

Supplementary Materials: The following supporting information can be downloaded at: https://www.mdpi.com/article/10.3390/coatings13071249/s1, Figure S1: X-ray diffraction pattern of composite coating on VT1-0 titanium.

Author Contributions: Conceptualization, D.V.M. and K.V.N.; methodology, S.N.S. and E.A.B.; validation, D.V.M., K.V.N. and I.M.I.; formal analysis, E.A.B. and S.N.S.; investigation, M.A.P. and A.I.P.; resources, S.V.G.; writing—original draft preparation, A.I.P. and M.A.P.; writing—review and editing, D.V.M., I.M.I. and K.V.N.; visualization, A.I.P. and I.M.I.; supervision, S.L.S.; project administration, S.V.G. and S.V.G.; funding acquisition, D.V.M. and K.V.N. All authors have read and agreed to the published version of the manuscript.

Funding: The formation of coatings, as well as SEM, EDS, and XRD analyzes was supported by Russian Science Foundation grant No. 22-73-10149, https://rscf.ru/project/22-73-10149/ (accessed on 28 July 2022). The electrochemical studies and wettability measurements was supported by the Russian Science Foundation grant No. 23-13-00329, https://rscf.ru/project/23-13-00329/ (accessed on 15 May 2022).

Data Availability Statement: The data that support the findings of this study are available from the corresponding author upon reasonable request.

Conflicts of Interest: The authors declare no conflict of interest.

References

1. Mashtalyar, D.V.; Nadaraia, K.V.; Imshinetskiy, I.M.; Belov, E.A.; Filonina, V.S.; Suchkov, S.N.; Sinebryukhov, S.L.; Gnedenkov, S.V. Composite coatings formed on Ti by PEO and fluoropolymer treatment. *Appl. Surf. Sci.* **2021**, *536*, 147976. [CrossRef]
2. Aliofkhazraei, M.; Macdonald, D.D.; Matykina, E.; Parfenov, E.V.; Egorkin, V.S.; Curran, J.A.; Troughton, S.C.; Sinebryukhov, S.L.; Gnedenkov, S.V.; Lampke, T.; et al. Review of plasma electrolytic oxidation of titanium substrates: Mechanism, properties, applications and limitations. *Appl. Surf. Sci. Adv.* **2021**, *5*, 100121. [CrossRef]
3. Lingwei, M.; Wang, J.; Zhang, D.; Huang, Y.; Huang, L.; Wang, P.; Qian, H.; Li, X.; Terryn, H.A.; Mol, J.M. Dual-Action Self-Healing Protective Coatings with Photothermal Responsive Corrosion Inhibitor Nanocontainers. *Chem. Eng. J.* **2021**, *404*, 127118.
4. Del Olmo, R.; López, E.; Matykina, E.; Tiringer, U.; Mol, J.M.C.; Mohedano, M.; Arrabal, R. Hybrid PEO/sol-gel coatings loaded with Ce for corrosion protection of AA2024-T3. *Prog. Org. Coat.* **2023**, *182*, 107667. [CrossRef]
5. Ren, S.; Cui, M.; Liu, C.; Wang, L. A comprehensive review on ultrathin, multi-functionalized, and smart graphene and graphene-based composite protective coatings. *Corros. Sci.* **2023**, *212*, 110939. [CrossRef]
6. Liu, T.; Ma, L.; Wang, X.; Wang, J.; Qian, H.; Zhang, D.; Li, X. Self-healing corrosion protective coatings based on micro/nanocarriers: A review. *Corros. Commun.* **2021**, *1*, 18–25. [CrossRef]
7. Gnedenkov, S.V.; Sinebryukhov, S.L.; Mashtalyar, D.V.; Nadaraia, K.V.; Kiryukhin, D.P.; Kichigina, G.A.; Kushch, P.P.; Buznik, V.M. Composite coatings formed on the PEO-layers with the use of solutions of tetrafluoroethylene telomers. *Surf. Coat. Technol.* **2018**, *346*, 53–62. [CrossRef]
8. Kaseem, M.; Fatimah, S.; Nashrah, N.; Ko, Y.G. Recent progress in surface modification of metals coated by plasma electrolytic oxidation: Principle, structure, and performance. *Prog. Mater. Sci.* **2020**, *117*, 100735. [CrossRef]
9. Mashtalyar, D.V.; Nadaraia, K.V.; Sinebryukhov, S.L.; Gnedenkov, S.V. Protective Composite Coatings Formed on Mg Alloy Surface by PEO Using Organofluorine Materials. *J. Mater. Sci. Technol.* **2017**, *33*, 661–667. [CrossRef]
10. Xu, K.; Yang, Z.; Sun, W.; Wang, L.; Fan, J.; Zhang, H.; Wu, T.; Yu, S.; Nie, X.; Li, W.; et al. Acid permeability related corrosion protection properties of PTFE coatings for waste heat recovery. *Corros. Sci.* **2023**, *218*, 111141. [CrossRef]
11. Tsai, D.-S.; Tsai, Y.-C.; Chou, C.-C. Corrosion passivation of magnesium alloy with the duplex coatings of plasma electrolytic oxidation and tetrafluoroethylene-based polymers. *Surf. Coat. Technol.* **2019**, *366*, 15–23. [CrossRef]

12. Wang, K.; Xiong, D. Construction of lubricant composite coating on Ti6Al4V alloy using micro-arc oxidation and grafting hydrophilic polymer. *Mater. Sci. Eng. C.* **2018**, *90*, 219–226. [CrossRef] [PubMed]
13. Küçükosman, R.; Şüküroğlu, E.E.; Totik, Y.; Şüküroğlu, S. Investigation of wear behavior of graphite additive composite coatings deposited by micro arc oxidation-hydrothermal treatment on AZ91 Mg alloy. *Surf. Interfaces* **2021**, *22*, 100894. [CrossRef]
14. Ivanou, D.K.; Starykevich, M.; Lisenkov, A.D.; Zheludkevich, M.L.; Xue, H.B.; Lamaka, S.V.; Ferreira, M.G.S. Plasma anodized ZE41 magnesium alloy sealed with hybrid epoxy-silane coating. *Corros. Sci.* **2013**, *73*, 300–308. [CrossRef]
15. Nadaraia, K.V.; Suchkov, S.N.; Imshinetskiy, I.M.; Mashtalyar, D.V.; Kosianov, D.Y.; Belov, E.A.; Sinebryukhov, S.L.; Gnedenkov, S.V. New superhydrophobic composite coatings on Mg-Mn-Ce magnesium alloy. *J. Magnes. Alloy.* **2023**, *11*, 1721–1739. [CrossRef]
16. Gnedenkov, S.V.; Khrisanfova, O.A.; Sinebryukhov, S.L.; Puz', A.V.; Gnedenkov, A.S. Composite Protective Coating on Nitinol Surface. *Mater. Manuf. Process.* **2008**, *23*, 879–883. [CrossRef]
17. Gnedenkov, S.V.; Sinebryukhov, S.L.; Mashtalyar, D.V.; Egorkin, V.S.; Tsvetnikov, A.K.; Minaev, A.N. Composite Polymer-Containing Protective Layers on Titanium. *Prot. Met.* **2008**, *44*, 704–709. [CrossRef]
18. Gnedenkov, S.V.; Sinebryukhov, S.L. Composite Polymer Containing Coatings on the Surface of Metals and Alloys. *Corros. Sci.* **2009**, *16*, 387–405. [CrossRef]
19. Mashtalyar, D.V.; Gnedenkov, S.V.; Sinebryukhov, S.L.; Nadaraia, K.V. Formation of the composite coatings as a method of restoration of titanium products after exploration. *Non-Ferrous Met.* **2017**, *42*, 8–11. [CrossRef]
20. Gnedenkov, S.V.; Vovna, V.I.; Gordienko, P.S.; Sinebryukhov, S.L.; Cherednichenko, A.I.; Shchukarev, A.V. Chemical Composition of Antifriction Micro-arc Oxide Coating on Titanium Alloy BT16. *Prot. Met.* **2001**, *37*, 192–196. [CrossRef]
21. Zhu, M.; Song, Y.; Liu, Z.; Xu, D.; Dong, K.; Han, E.H. Optimization of thermal control and corrosion resistance of PEO coatings on 7075 aluminum alloy by frequency alteration. *Surf. Coat. Technol.* **2022**, *446*, 128797. [CrossRef]
22. Gnedenkov, S.V.; Sinebryukhov, S.L. Electrochemical Impedance Spectroscopy of Oxide Layers on the Titanium Surface. *Russ. J. Electrochem.* **2005**, *41*, 858–865. [CrossRef]
23. Gnedenkov, S.V.; Sinebryukhov, S.L.; Sergienko, V.I. Electrochemical Impedance Simulation of a Metal Oxide Heterostructure/Electrolyte Interface: A Review. *Rus. J. Electrochem.* **2006**, *42*, 197–211. [CrossRef]
24. Sharifi, H.; Aliofkhazraei, M.; Darband, G.B.; Rouhaghdam, A.S. Characterization of PEO nanocomposite coatings on titanium formed in electrolyte containing atenolol. *Surf. Coat. Technol.* **2016**, *304*, 438–449. [CrossRef]
25. Sopchenski, L.; Popat, K.; Soares, P. Bactericidal activity and cytotoxicity of a zinc doped PEO titanium coating. *Thin Solid Film.* **2018**, *660*, 477–483. [CrossRef]
26. Santos-Coquillat, A.; Mohedano, M.; Martinez-Campos, E.; Arrabal, R.; Pardo, A.; Matykina, E. Bioactive multi-elemental PEO-coatings on titanium for dental implant applications. *Mater. Sci. Eng. C* **2019**, *97*, 738–752. [CrossRef]
27. Liu, Y.; Zheng, Y.; Chen, X.-H.; Yang, J.-A.; Pan, H.; Chen, D.; Wang, L.; Zhang, J.; Zhu, D.; Wu, S.; et al. Fundamental Theory of Biodegradable Metals—Definition, Criteria, and Design. *Adv. Funct. Mater.* **2019**, *29*, 1805402. [CrossRef]
28. Gu, Y.; Chen, C.F.; Bandopadhyay, S.; Ning, C.; Zhang, Y.; Guo, Y. Corrosion mechanism and model of pulsed DC microarc oxidation treated AZ31 alloy in simulated body fluid. *Appl. Surf. Sci.* **2012**, *258*, 6116–6126. [CrossRef]
29. Castellanos, A.; Altube, A.; Vega, J.M.; García-Lecina, E.; Díez, J.A.; Grande, H.J. Effect of different post-treatments on the corrosion resistance and tribological properties of AZ91D magnesium alloy coated PEO. *Surf. Coat. Technol.* **2015**, *278*, 99–107. [CrossRef]
30. Staicopolus, D.N. The computation of surface tension and of contact angle by the sessile-drop method. *J. Colloid Sci.* **1962**, *17*, 439–447. [CrossRef]
31. Erbil, H.Y. The debate on the dependence of apparent contact angles on drop contact area or three-phase contact line: A review. *Surf. Sci. Rep.* **2014**, *69*, 325–365. [CrossRef]
32. Viades-Trejo, J.; Gracia-Fadrique, J. Spinning drop method: From Young–Laplace to Vonnegut. *Colloids Surf. A Physicochem. Eng. Asp.* **2007**, *302*, 549–552. [CrossRef]
33. Fronzi, M.; Assadi, M.; Hanaor, D. Theoretical insights into the hydrophobicity of low index CeO2 surfaces. *Appl. Surf. Sci.* **2019**, *478*, 68–74. [CrossRef]
34. Cassie, A.B.D.; Baxter, S. Wettability of porous surfaces. *Trans. Faraday Soc.* **1944**, *40*, 546–551. [CrossRef]

Disclaimer/Publisher's Note: The statements, opinions and data contained in all publications are solely those of the individual author(s) and contributor(s) and not of MDPI and/or the editor(s). MDPI and/or the editor(s) disclaim responsibility for any injury to people or property resulting from any ideas, methods, instructions or products referred to in the content.